SLAC-PUB-1150
(ACC)
November 1972

BEAM FEEDBACK ELECTRONICS FOR THE SPEAR STORAGE RING*

Jean-Louis Pellegrin

Stanford Linear Accelerator Center
Stanford University, Stanford, California 94305

ABSTRACT

The two beams of the 2 GeV Stanford electron-positron storage ring can exhibit, under certain modes of operation, coherent oscillations which have a rate of growth proportional to the beam current. Since this rate is much slower than the machine revolution frequency, it is possible to produce damping by means of negative feedback, the beam itself being part of the feedback loop. Three systems have been built, two for the damping of transverse oscillations at the betatron frequency, and one for the damping of longitudinal oscillations at the synchrotron frequency. The electronics for these systems require wide band high power amplifiers and nanosecond circuitry.

(Submitted to Nucl. Instr. and Methods.)

---

*Work supported by the U. S. Atomic Energy Commission.

1. Introduction

The main parameters of the Stanford positron-electron storage ring SPEAR are found in Ref. 1. A theory for the damping of beam coherent instabilities has been studied by a number of authors,[2, 3, 4] and some machines have been equipped with systems of the same nature as the one we are about to describe.

If one neglects phase shifts at the oscillation frequency and also radiation damping, a model for growing, coherent beam oscillations can be the RLC circuit of Fig. 1 where the resistance has been allowed to be negative in order to create antidamping. The differential equation for the closed loop circuit is

$$C\frac{dV}{dt} - \frac{V}{R} + \frac{1}{L}\int V\,dt = -G\frac{V}{r} \tag{1}$$

or

$$\ddot{V} + \left(\frac{G}{rC} - \frac{1}{RC}\right)\dot{V} + \frac{V}{LC} = 0 \tag{2}$$

when the gain is large enough, that is $G \geq \frac{r}{R}$, the solution is nongrowing.

The general method proposed for damping beam transverse coherent oscillations consists in detecting the beam displacement Δx from the equilibrium orbit, and after one revolution and suitable amplification, exciting the beam in antiphase. In terms of the equation of a well behaved undamped motion

$$\Delta\ddot{x} - \frac{2}{\tau_1}\Delta\dot{x} + \omega_b^2\,\Delta x = 0 \tag{3}$$

in which Δx would be some transverse displacement of the bunch center-of-mass, $\frac{1}{\tau_1}$ a rate of antidamping and ω_b the betatron natural frequency, the damping mechanism is achieved by applying to (3) a forcing function of the form $-\frac{2\Delta\dot{x}}{\tau_2}$ where $\frac{1}{\tau_2}$ is a damping rate proportional to the loop gain. Once more, for

sufficient gain the solution becomes nongrowing. We note however, that besides the delay of one revolution required by the system to operate (790 nsec for SPEAR), and maybe a 180^{o} phase shift for negative feedback purpose, a 90^{o} phase shift at $\omega=\omega_b$ is necessary between detection and excitation, i.e., between pickup and feedback, since we detect a quantity proportional to Δx and we feedback a quantity proportional to $\Delta\dot{x}$. This phase shift is readily obtained for the transverse beam feedback because the machine stability requires a tune of approximately 5.25, that is $\omega_b = 5.25\ \Omega_0$ where Ω_0 is the revolution frequency. Consequently the pickup and feedback stations can be located next to each other.

In the case of the longitudinal feedback, if one assumes very small departures $\Delta\phi$, of the phase of the bunch center-of-mass, from the synchronous phase, Eq. (3) can be replaced by

$$\Delta\ddot{\phi} - \frac{2}{\tau_3}\,\Delta\dot{\phi} + \omega_s^2\,\Delta\phi = 0 \qquad (4)$$

with $1/\tau_3$ a rate of antidamping and ω_s the synchrotron oscillation frequency. Like for the betatron motion we describe the phenomenon of energy oscillation with a linear model, but are certainly not attempting to explain what is the driving force of such oscillations. The energy deviation ΔE is proportional to $\Delta\dot{\phi}$ and is directly measured as a beam radial displacement. Therefore no extra phase shift is required, except the usual 180^{o} for negative feedback. Figure 2 is a sketch of the principle of both systems.

Before studying the mechanism used for the detection of beam oscillations at the betatron and synchrotron frequencies, we will describe the mode of coupling to and from the beam, and first, the beam itself.

2. The Detection of Beam Oscillations

2.1 The SPEAR beam

Each beam is made of a short bunch of particles revolving around the machine at the frequency $F_0 = 1.28\ 10^6$ Hz. The bunch charge distribution is Gaussian and the instantaneous current through a plane perpendicular to the beam, turns out to be Gaussian also; it can be expressed as

$$i = I_p\, e^{-\frac{c^2 t^2}{2\sigma^2}} \tag{5}$$

with I_p peak beam current; σ longitudinal half-bunch length; $\sigma = 14$ cm at 2 GeV. From Eq. (5) we calculate the peak and the rms currents of each beam as a function of the average current

$$I_p = i_{av}\, \frac{\sqrt{2\pi}\, c}{\sigma \omega_0} = 670\ i_{av} \tag{6}$$

$$I^2_{rms} = I_p i_{av}\, \frac{1}{\sqrt{2}} = 474\ i^2_{av} \tag{7}$$

Relations (6) and (7) are useful to calculate the amplitude of the signals and the power induced by the beam into the pickup electrodes.

2.2 Pickup and feedback electrodes

Four strip lines in a rectangular configuration (Fig. 3) are used to sense the vertical and horizontal beam oscillations. An identical set of strip lines, but three times longer, serves the purpose of feedback electrodes. Masking of the horizontal outside electrodes from the synchrotron radiation is done with water-cooled aluminum masks; the electrical symmetry of the structure is restored by installing dummy masks on the masks' opposite sides. It has been shown[5] that a strip line coupled to a beam constitutes a wide band circuit and yields signals which are a good reproduction of the beam charge distribution.

The geometry of Fig. 3 was found to have the following parameters:

$$\begin{aligned} &\text{Common mode voltage} && V_{1,2} = 4 \text{ volt/peak A} \\ &\text{Differential mode voltage} && V_1 - V_2 = 80 \text{ volt/peak A, m} \\ &\text{(Sensitivity } A_p\text{)} \end{aligned} \tag{8}$$

These signals were measured at the upstream ports 1 and 2, with all terminals connected to a matched load (50 Ω). It should be noted that this structure presents some directivity, that is, the signals propagating out of the downstream ports are much smaller than the signal observed at the upstream ports. Figure 4 shows the response of a 100 cm strip line to a SPEAR positron beam of 33 mA average. The electrode dimensions are the same as those of Fig. 3. The bipolar nature of the pulse is not due to a differentiation but is an intrinsic property of this type of pickup; the positive pulse is induced as the beam fields sweep the upstream port discontinuity, and the negative pulse is induced when these fields sweep the downstream port discontinuity; therefore the time difference between them is approximately equal to twice the propagation time along the strip line.

The power coupled by the beam to one strip line terminal is found to be 315 watt/A^2 of average current. Thus for the SPEAR design current of 250 mA per beam each terminal will deliver 19 watts.

2.3 The detection circuit

The algebraic difference between two opposite electrode voltages yields a train of bipolar pulses at the frequency F_0, which constitutes an amplitude modulated carrier. The modulation components are dependent on the beam current and some of them are identified as:

a) a dc component due to residual equilibrium orbit distortions. Indeed the beams are allowed horizontal and vertical excursions

of ± 1 cm, and as a result this component can be very large; since it would saturate the feedback loop amplifier it must be eliminated.

b) a family of terms at frequencies $\omega_{bn} = (\nu \pm n)\,\Omega_0$. These components are a result of coherent betatron oscillations; for $n=5$, the lowest frequency is in general between 200 and 400 kHz.

c) The horizontal pickup electrodes can also indicate a modulation at the synchrotron frequency, $\omega_s \approx 7$ kHz, which corresponds to bunch energy variations.

The circuit of Fig. 5 was devised to sort out the wanted from the unwanted signals. A pair of rf variable attenuators are controlled by a low frequency servo which insures that no dc component subsists in the loop output. The purpose of the double integrator is precisely to restore the dc component (the loop error signal) and, while preserving the carrier at $\omega = \Omega_0$, to widen the pulses to make them suitable for the betatron feedback amplifier.

The sampler does away with the carrier, and after proper filtering, produces the cw synchrotron oscillation. If the synchrotron feedback were not operating, the horizontal betatron signals would exhibit a modulation at $\omega = \omega_b \pm n\omega_s$. An alternative could be to remove all filtering beyond the sampler and let the variable attenuators' control operate up to $\omega = \omega_s$. However these are PIN diode attenuators and their bias cannot easily be controlled at hundreds of kilocycle rates.

Figure 6 describes the operation of the attenuators; they are of a reflective type which requires that the other end of the strip line pickup be terminated. The UM4300 diode has 60 watts dissipation capability and can very well handle the maximum attenuator dissipation.

3. Transverse Beam Feedback System

3.1 Amplifier specifications

The transverse beam feedback as described by Eq. (3) demands that we apply to the beam a transverse momentum Δp proportional to a displacement Δx. The force on a particle is 2 ecB, where B is the magnetic induction due to the current in the feedback electrode, and the factor 2 accounts for the effect of the electric field associated with B. We have

$$B = \frac{\mu_0 i}{\pi d} = \frac{\mu_0}{\pi d} \frac{I_p A_p G}{R} \Delta x \tag{9}$$

i current applied to feedback electrode

$d = 0.18$ m, feedback electrodes spacing

I_p peak beam current

$A_p = 80$ V/A m, pickup electrode sensitivity

G amplifier gain

$R = 50\ \Omega$, impedance of pickup electrodes

Δx beam transverse displacement from equilibrium orbit

Since the tune of the ring is $\nu = 5.25$, we have

$$\int \Delta x \, dt \Big|_{\substack{\text{pickup} \\ \text{location}}} = \frac{\Delta x}{\omega_b} \Big|_{\substack{\text{feedback} \\ \text{location}}} \tag{10}$$

then the transverse momentum at the feedback location is found to be $\frac{2\,ecB}{\omega_b}$, and since the beam experiences that momentum only every other turn, we get

$$\frac{\Delta p}{p} = \frac{ecB}{p\omega_b} \frac{\ell}{c} F_0 \tag{11}$$

where ℓ is the length of the feedback strip line, and F_0 is the revolution frequency.

Introducing (11) and (9) into Eq. (3), we have

$$\frac{1}{c}\left[\Delta\ddot{x} - \frac{2}{\tau_1}\Delta\dot{x} + \omega_b^2\Delta x\right] = -\frac{e\mu_0 \ell I_p A_p G F_0}{p\pi d R \omega_b}\Delta\dot{x} \tag{12}$$

where the minus sign on the right is necessary for negative feedback.

The condition for a damped solution is then

$$\tau_2 = \frac{2pc\,\pi d R\omega_b}{e\,c^2\mu_0 \ell I_p A_p G F_0} < \tau_1 \tag{13}$$

It was felt that no coherent instability would develop for peak currents less than 1 ampere (about 2 mA average current), and that their time constant would be perhaps of the order of few tens of millisecond. If we pick $\tau_2 = 3\ 10^{-3}$ sec, and with

$$pc = 2\ 10^9 \text{ eV}$$

$$\ell = 1 \text{ m}$$

$$I_p = 1 \text{ A}$$

$$F_0 = 1.28\ 10^6 \text{ sec}^{-1}$$

$$\omega_b = 2\pi \times 5.25\ F_0$$

we get $G = 138$.

Assuming a residual oscillation of $\pm \frac{1}{4}$ mm for the maximum SPEAR average current of 250 mA, we calculate the amplifier output as ± 460 volts.

The amplifier bandwidth was determined having in mind to feedback possibly on two consecutive bunches which are 20 nsec apart; also, a large bandwidth was desirable in order to keep the duty cycle low, and consequently also the output power. One last requirement was that the amplifier output impedance should be approximately matched to the electrode impedance in order to absorb the power coupled from the beam.

3.2 Chain amplifier

The sketch of a transverse feedback system is shown on Fig. 7; the same set of feedback electrodes is used for both beams. Yet, since the beams do not cross at this location, the detection circuits are gated "on" at different times. The table of Fig. 8 lists the main characteristics of the amplifiers constituting the chain. Operation is class AB throughout, that is, all outputs and inputs are monopolar, but the preamplifier (Figs. 9 and 10) accepts bipolar inputs and has one inverting output, and one noninverting output. As a result, each electrode is driven by a separate chain. All circuits use additive amplification in order to achieve the large peak power required and maintain wide band response. The low level and medium level amplifiers use printed circuit traces for the inductances of their delay lines (Fig. 11). Their circuit is quite similar to the circuit of the high level amplifier (Fig. 12). One should note that the power dissipated in the high level amplifier dummy load can be quite high, since it absorbs the amplifier's backward wave, the opposite amplifier's forward wave and finally the beam induced power.

4. Longitudinal Beam Feedback System

4.1 Amplifier specifications

Equation (4) can be modified to include the effect of feedback; it becomes

$$\frac{E_0}{\omega_{rf}} \left[\Delta\ddot{\phi} - \frac{2}{\tau_3} \Delta\dot{\phi} + \omega_s^2 \Delta\phi \right] = \Delta P \qquad (14)$$

with E_0 the beam nominal energy, ω_{rf} the frequency of the rf system and $\frac{1}{\tau_3}$ a rate of antidamping. ΔP is the power feedback to the beam as a function of the energy deviation ΔE of the bunch.

$$\Delta P = \Delta x \, A_p I_p G e F_0 \qquad (15)$$

Δx is the radial displacement due to ΔE, and the other symbols are the same as for the betatron feedback. At the pickup location s_p, the beam displacement is related to the energy deviation through the off-energy function $\eta(s)$, and the relative energy deviation is related to $\Delta\dot{\phi}$ through the momentum compaction factor α; we have from Ref. 6.

$$\Delta x|_{s=s_p} = \eta(s_p)\,\frac{\Delta E}{E_0} = -\eta(s_p)\,\frac{\Delta\dot{\phi}}{\alpha\omega_{rf}} \tag{16}$$

Then (14) becomes

$$\Delta\ddot{\phi} - \frac{2}{\tau_3}\,\Delta\dot{\phi} + \omega_s^2\,\Delta\phi = -\frac{e\eta A_p I_p G F_0}{E_0 \alpha}\,\Delta\dot{\phi} \tag{17}$$

A value for τ_3 is not yet available, nevertheless we evaluate the damping time constant τ_4, of a practical system, using the following assumptions:

$$I_p = 1\ A$$

$$G = 200$$

$$\alpha = 0.038$$

$$\eta = 2\ m$$

it comes

$$\tau_4 = \frac{2E_0\alpha}{e\eta\, A_p I_p G F_0} = 30\ \text{msec} \tag{18}$$

Then for a residual energy deviation of $\pm 0.02\%$ we calculate from (16) a radial displacement of ± 0.4 mm and for the full SPEAR beam, the maximum amplifier output should be ± 1070 volts.

4.2 Bipolar chain amplifier

Figure 13 is a block diagram of the longitudinal beam feedback system. Note that since the synchrotron oscillation frequency is so low compared to the

revolution frequency, no delay line is necessary, and the timing of the system is performed by selecting the proper triggers for the gate generators.

Some modifications were made to the chain amplifier in order to drive the energy gap with both polarities. Figure 14 shows that the twin high level stages of one system can be interconnected to make a bipolar amplifier. Also, by increasing the plate impedance, one can minimize grid loading and somewhat increase the output, at the expense of a bandwidth reduction. The plate line and the grid line were redesigned using the data of Ref. 7. All transformers are made out of 100 Ω twisted wire transmission lines.[8] As a result of the above modifications, the chain amplifier risetime increased to 12 nsec, but due to a better trading between tube current and voltage, the gain could be increased by 3 dB and the output to ± 600 volts into a matched load. Yet, twice this voltage is available if the amplifier is unterminated, so we turn now to the study of the load presented by the gap.

4.3 Circuit of the energy feedback gap

The ceramic gap is 1" wide on an 8" diam tube; its capacity is approximately 20 pF. The metal frame securing the gap constitutes a dc short circuit, but by stacking ferrite blocks around the beam pipe the inductance of the circuit can be increased to 0.5 μH.

A model for the gap is indicated on Fig. 15. The response to an input ramp $V_i = at$, for the case of critical damping, is:

$$V_0 = a\frac{L}{R}\left[1 - \left(1 - \frac{2R}{L}t\right)e^{-\frac{2R}{L}t}\right] \qquad (19)$$

The maximum $\frac{aL}{R}(1 + e^{-2})$ is obtained for $t = \frac{L}{R}$. Taking a ramp of 1200 volt/12 nsec, then

$$a = 100 \quad 10^9 \text{ V/sec}$$

and with

$R = 50\ \Omega$

$L = 0.5\ \mu H$

$C = 50$ pF (the gap capacity must be increased to achieve critical damping)

the gap voltage is found to reach 1135 volts after 10 nsec, a time slightly less than the chain amplifier risetime.

5. Conclusion and Results

Shortly after the first turn on of SPEAR, the operation of the transverse beam feedback was found to be effective in damping the residual betatron oscillations created by the kicker magnets during injection. The burst of these oscillations occurs at the filling rate of 20 Hz, and decays in about 20 msec under the effect of radiation damping; with the feedback "on", a damping rate of the order of 1 msec was observed; this agrees quantitatively with the calculation of Section 3.1. But the full evaluation of the system performance is closely related to the overall storage ring operation and remains outside the scope of this paper. The present status of SPEAR is reported in Ref. 9.

As of the present time, the longitudinal beam feedback has not been used. It is expected to interact to some extent with the transverse beam feedback,[10] and if this is the case, some modifications of the latter might be necessary.

ACKNOWLEDGEMENTS

It is a pleasure to thank Burton Richter and J. R. Rees, who headed the design and construction of SPEAR, for discussing, defining and evaluating this system. In addition, the author is very grateful to R. A. Scholl for his insight and encouragement in all aspects of this project, and to C. R. Carman for designing and testing many of its constituents. Gratefully acknowledged also are the development work of A. K. Chang on the chain amplifier, the electrode design of L. G. Karvonen and discussions with H. Wiedemann regarding the longitudinal beam feedback.

REFERENCES

1. SLAC Storage Ring Group, Proc. CERN Symposium on High Energy Accelerators, 1971.
2. B. Richter, Stanford Linear Accelerator Center, private communication, SPEAR-25 (March 1970).
3. G. H. Rees, NIRL/R/99, Rutherford High Energy Laboratory (March 1965).
4. M. Q. Barton, J. G. Cottingham and A. Tranis, Rev. Sci. Instr. 35 (1964) 624.
5. Q. A. Kerns, D. B. Large, Lawrence Radiation Laboratory, Report No. UCRL-11551 (July 1964).
6. M. Sands, Stanford Linear Accelerator Center, Report No. SLAC-121 (November 1970).
7. W. L. Gagnon and Bob H. Smith, IEEE Trans. Nucl. Sci. NS-16, 551 (1969).
8. C. Norman Winningstad, IRE Trans. Nuclear Sci. 6 (1959) 26.
9. SPEAR Storage Ring Group, Stanford Linear Accelerator Center, Report No. SLAC-PUB-1128 (October 1972).
10. M. Sands, Stanford Linear Accelerator Center, private communication, SPEAR-143 (June 1972).

FIGURE CAPTIONS

1. Beam feedback analogy.
2. Principle of transverse and longitudinal beam feedback.
3. Pickup electrodes geometry.
4. Response of a 100 cm strip line to a SPEAR positron beam of 33 mA average; 2 nsec/div., 20 volts/div.
5. Beam oscillations detection circuit.
6. Attenuation and dissipation of diode attenuator.
7. Transverse feedback scheme for two beams.
8. Chain amplifier characteristics.
9. Circuit diagram of pre-amplifier.
10. View of pre-amplifier.
11. View of printed circuit distributed amplifier and high level stage.
12. Circuit diagram of high level amplifier.
13. Block diagram of longitudinal feedback system for two beams.
14. Bipolar configuration of chain amplifier.
15. Gap response to a ramp excitation.

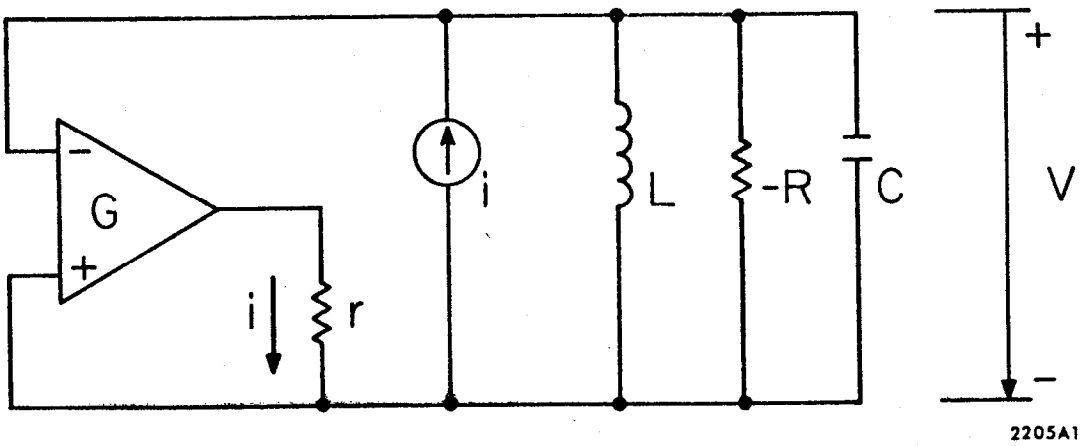

Fig. 1

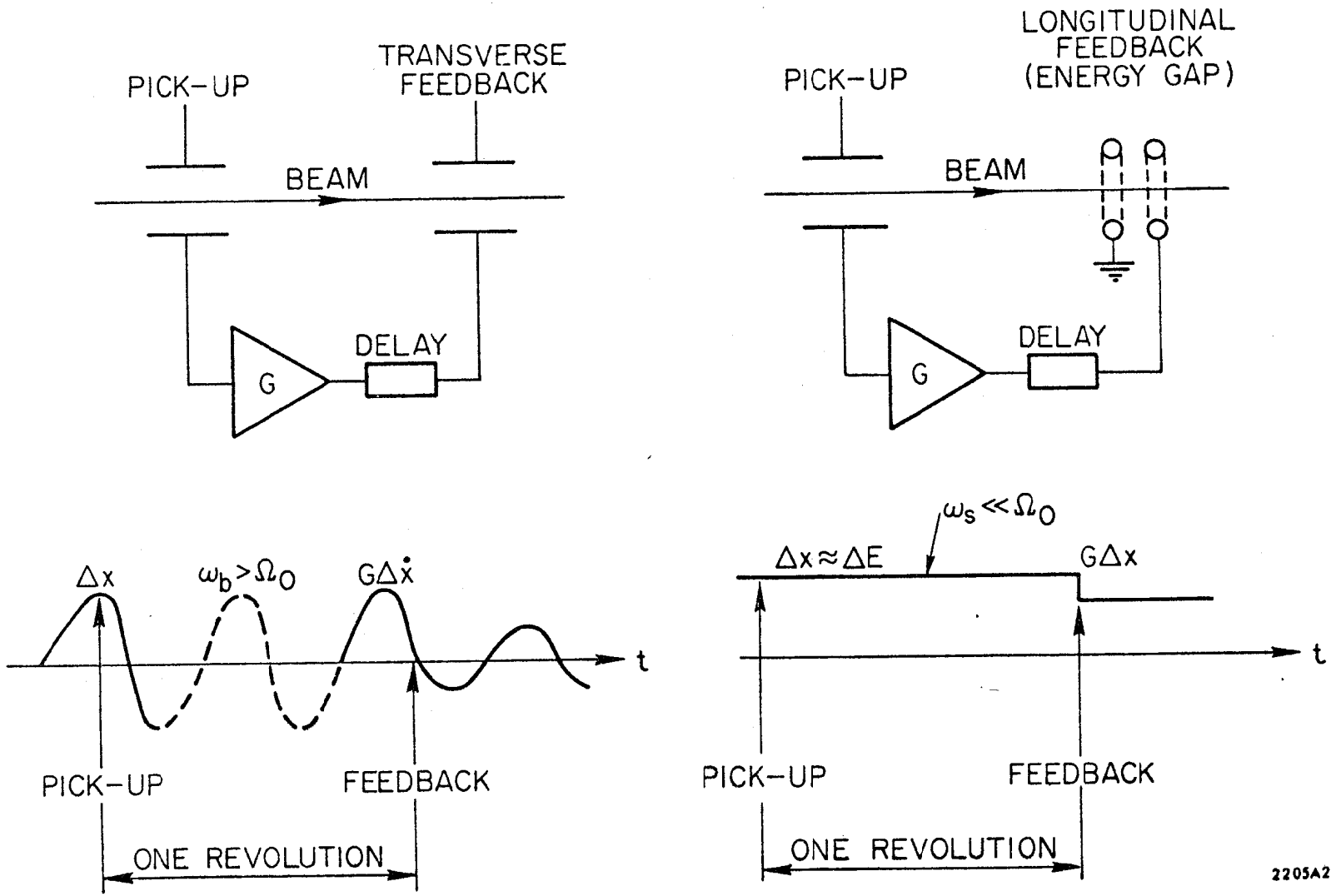
PICK-UP
TRANSVERSE FEEDBACK
BEAM
G
DELAY
LONGITUDINAL FEEDBACK (ENERGY GAP)
PICK-UP
BEAM
G
DELAY
Δx
ω_b > Ω_0
GΔẋ
t
PICK-UP
FEEDBACK
ONE REVOLUTION
ω_s ≪ Ω_0
Δx ≈ ΔE
GΔx
t
PICK-UP
FEEDBACK
ONE REVOLUTION
2205A2

Fig. 2

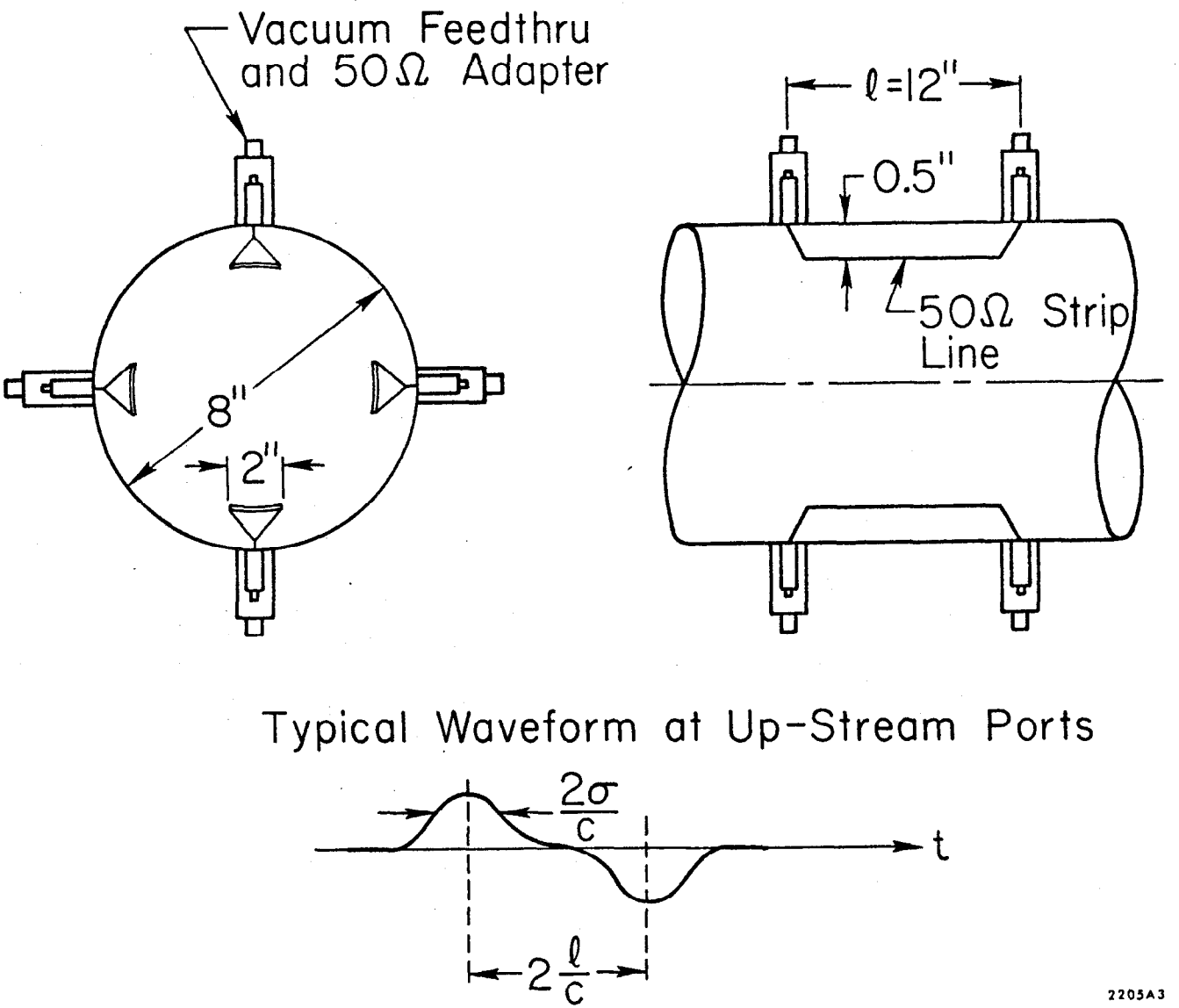
Vacuum Feedthru
and 50Ω Adapter
8"
2"
ℓ=12"
0.5"
50Ω Strip
Line
Typical Waveform at Up-Stream Ports
2σ/c
t
2ℓ/c
2205A3

Fig. 3

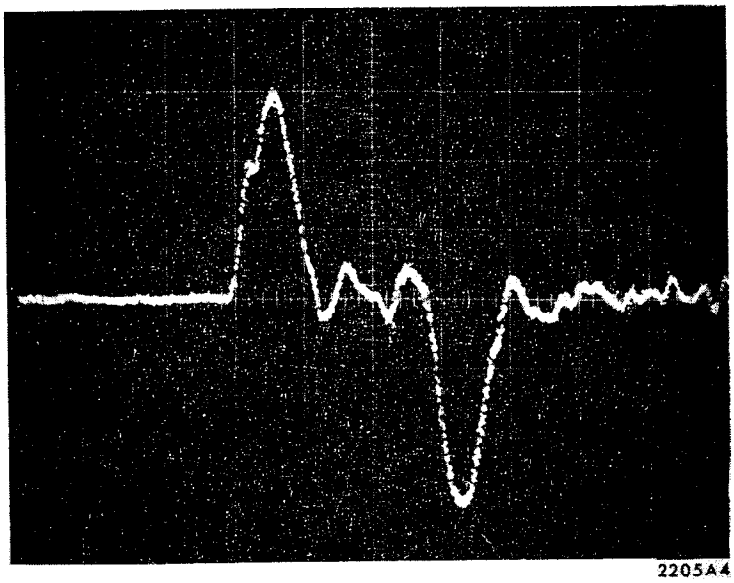

Fig. 4

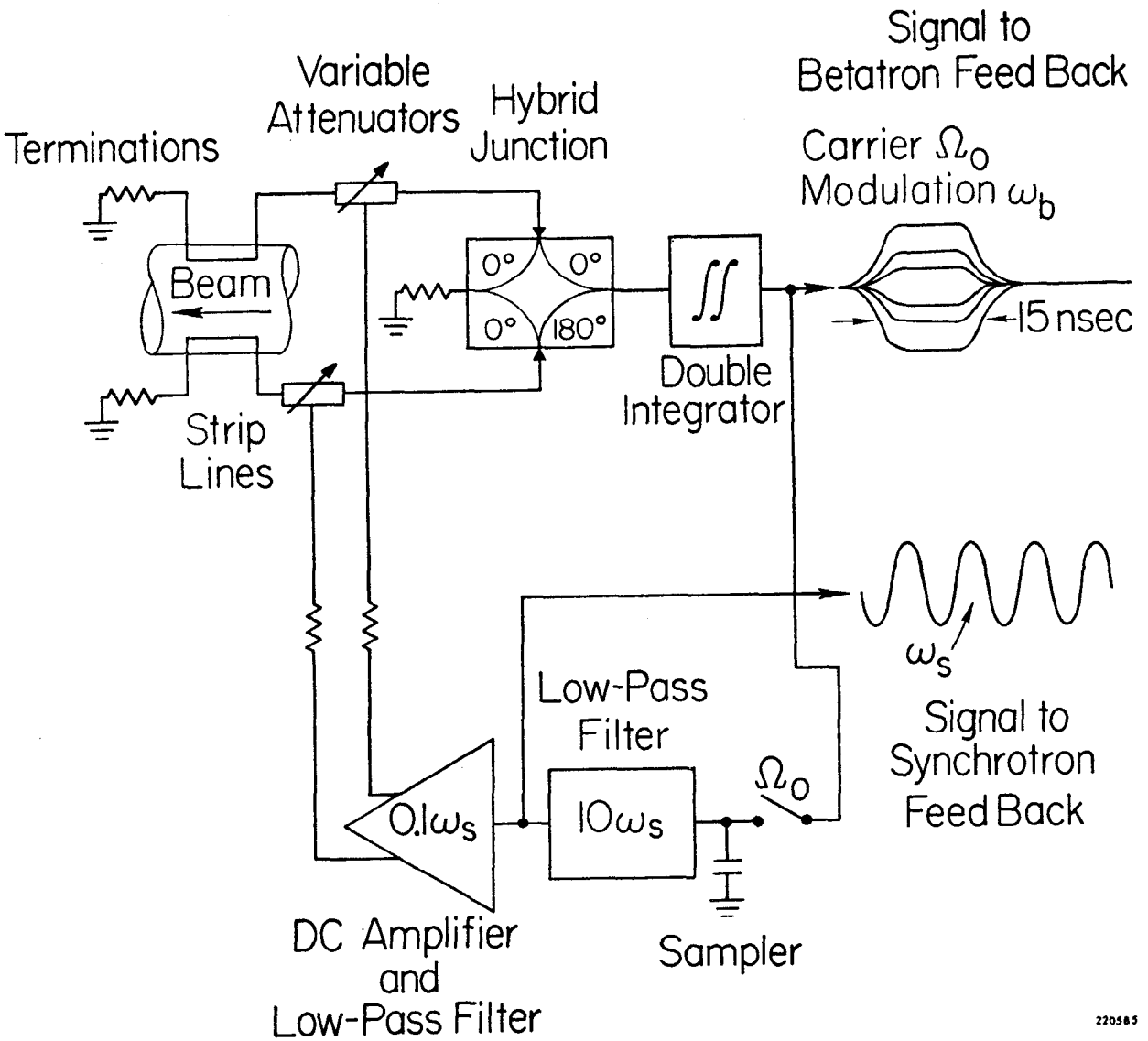
Signal to
Betatron Feed Back
Variable
Attenuators
Hybrid
Junction
Terminations
Carrier Ω_o
Modulation ω_b
Beam
0°
0°
0°
180°
15 nsec
Double
Integrator
Strip
Lines
ω_s
Low-Pass
Filter
Signal to
Synchrotron
Feed Back
Ω_o
$0.1\omega_s$
$10\omega_s$
DC Amplifier
and
Low-Pass Filter
Sampler
220585

Fig. 5

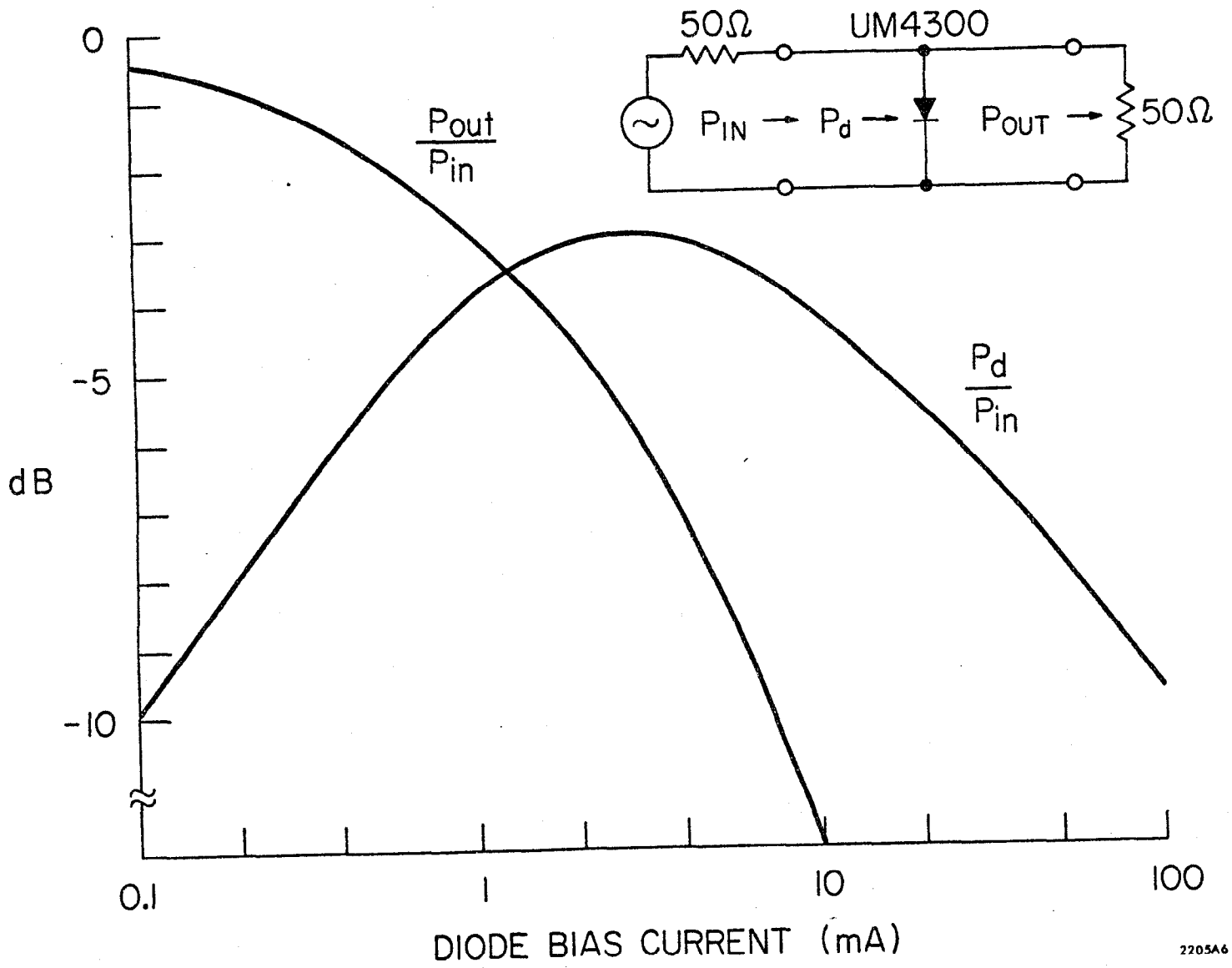
50Ω
UM4300
PIN
Pd
POUT
50Ω
Pout / Pin
Pd / Pin
0
-5
-10
dB
0.1
1
10
100
DIODE BIAS CURRENT (mA)
2205A6

Fig. 6

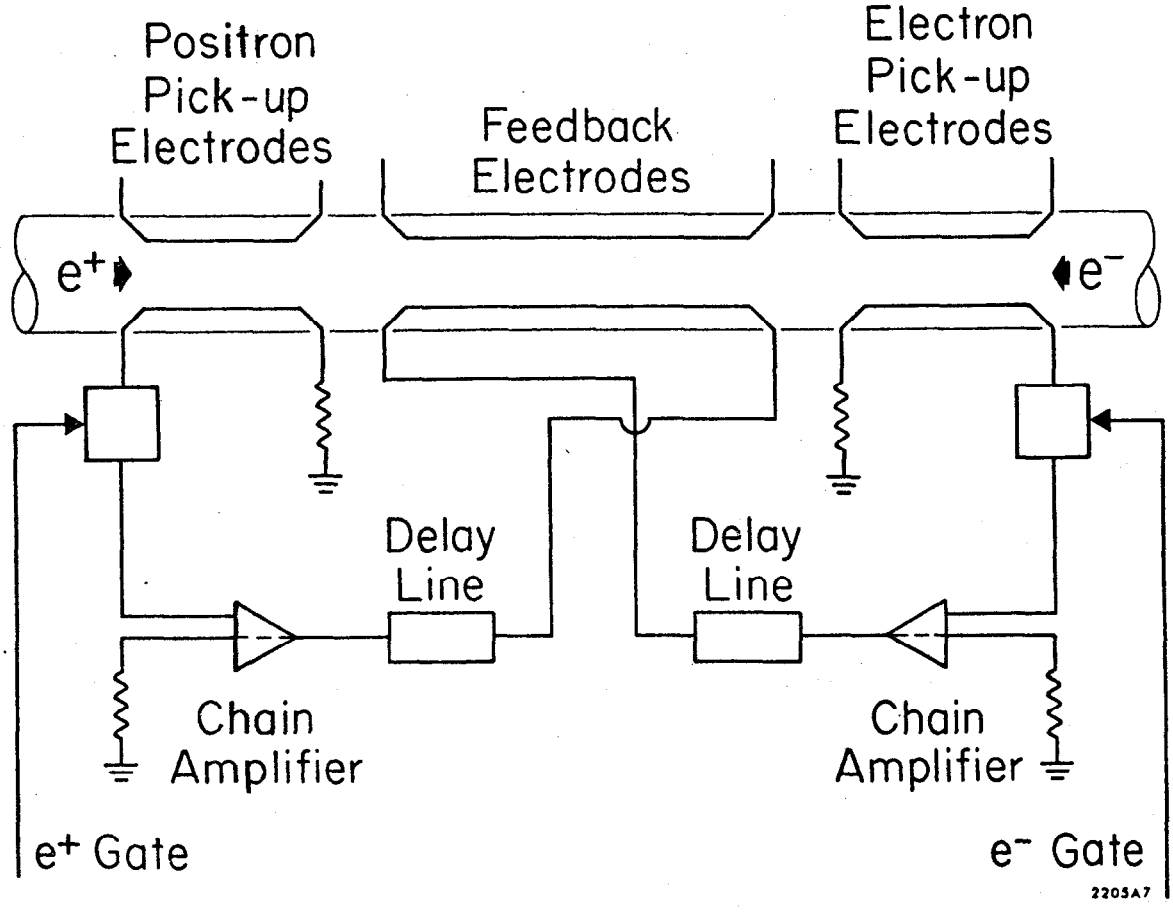
Positron
Pick-up
Electrodes
Feedback
Electrodes
Electron
Pick-up
Electrodes
e+
e−
Delay
Line
Delay
Line
Chain
Amplifier
Chain
Amplifier
e+ Gate
e− Gate
2205A7

Fig. 7

	High Level	Medium Level	Low Level	Pre-Amplifier
Number of stages	8	18	18	6 + 1
Type of active device	4CX250 Tetrode	7905 Pentode	7905 Pentode	2N2219/2N3866 Transistors
Type of fabrication	hand wired	printed circuit	printed circuit	printed circuit
Input/output impedance	50Ω	50Ω	50Ω	50Ω
Gain	10 dB	10 dB	10 dB	(14 + 14) dB
Output voltage	500 V	180 V	60 V	20 V
Risetime	5 nsec	5 nsec	5 nsec	3 nsec
Maximum average output power	200 watts	20 watts	--	--

FIG. 8

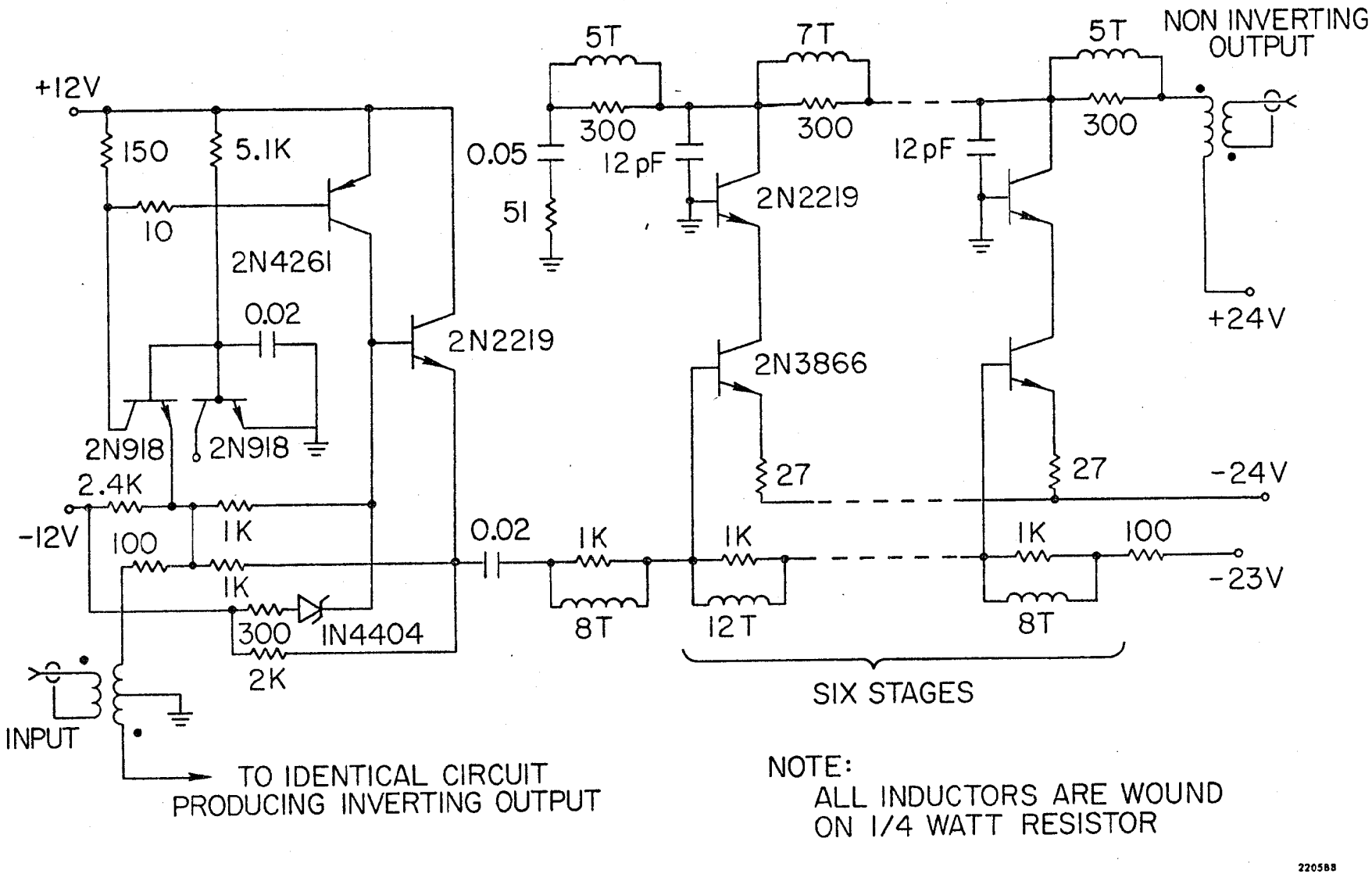
+12V
150
5.1K
10
2N4261
0.02
2N2219
2N918
2N918
2.4K
-12V
100
1K
1K
300
IN4404
2K
INPUT
TO IDENTICAL CIRCUIT
PRODUCING INVERTING OUTPUT
0.05
51
5T
300
12pF
2N2219
7T
300
2N3866
0.02
1K
8T
1K
12T
27
5T
300
12pF
NON INVERTING
OUTPUT
+24V
27
-24V
1K
100
-23V
8T
SIX STAGES
NOTE:
ALL INDUCTORS ARE WOUND
ON 1/4 WATT RESISTOR
220588

Fig. 9

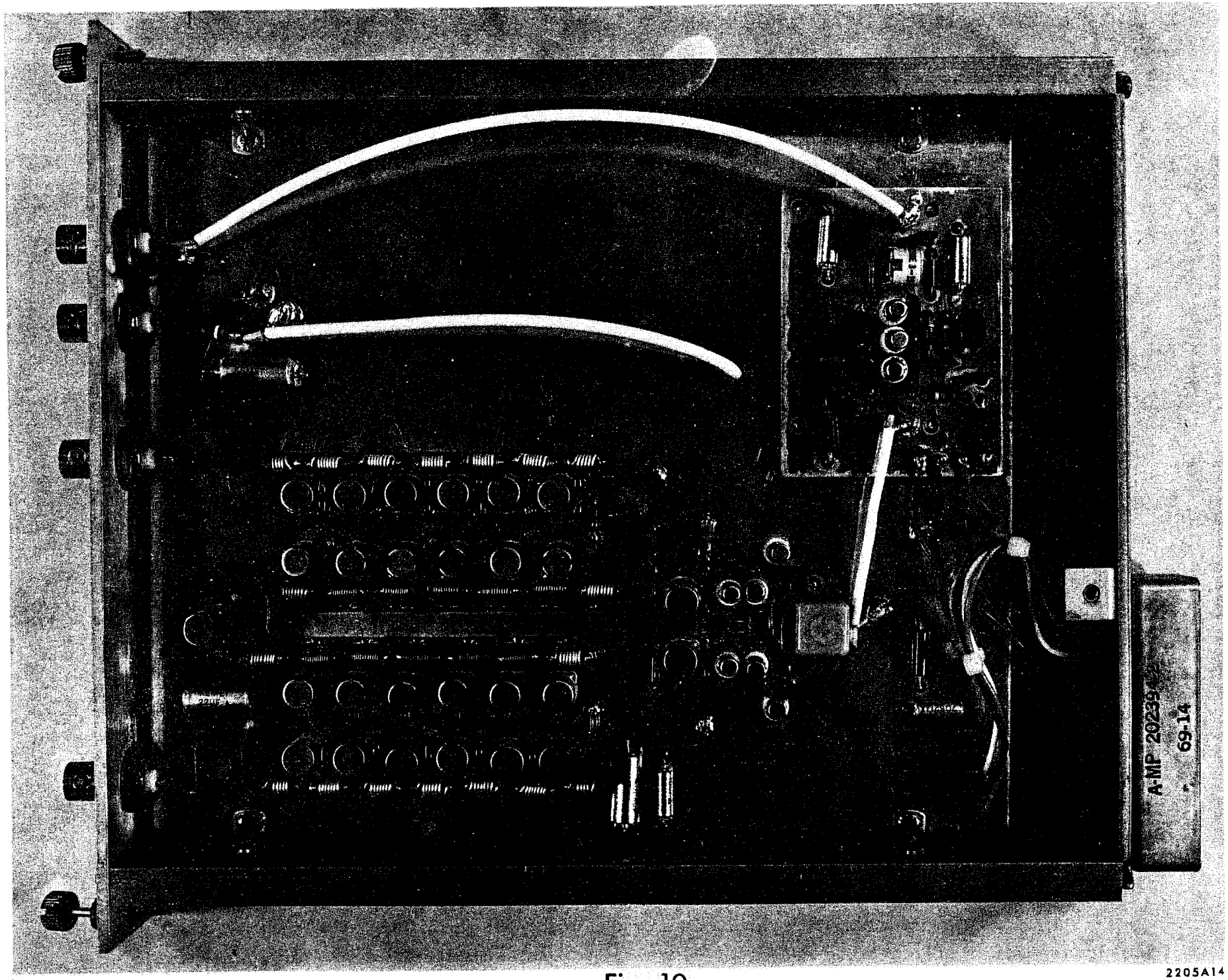

2205A14

Fig. 10

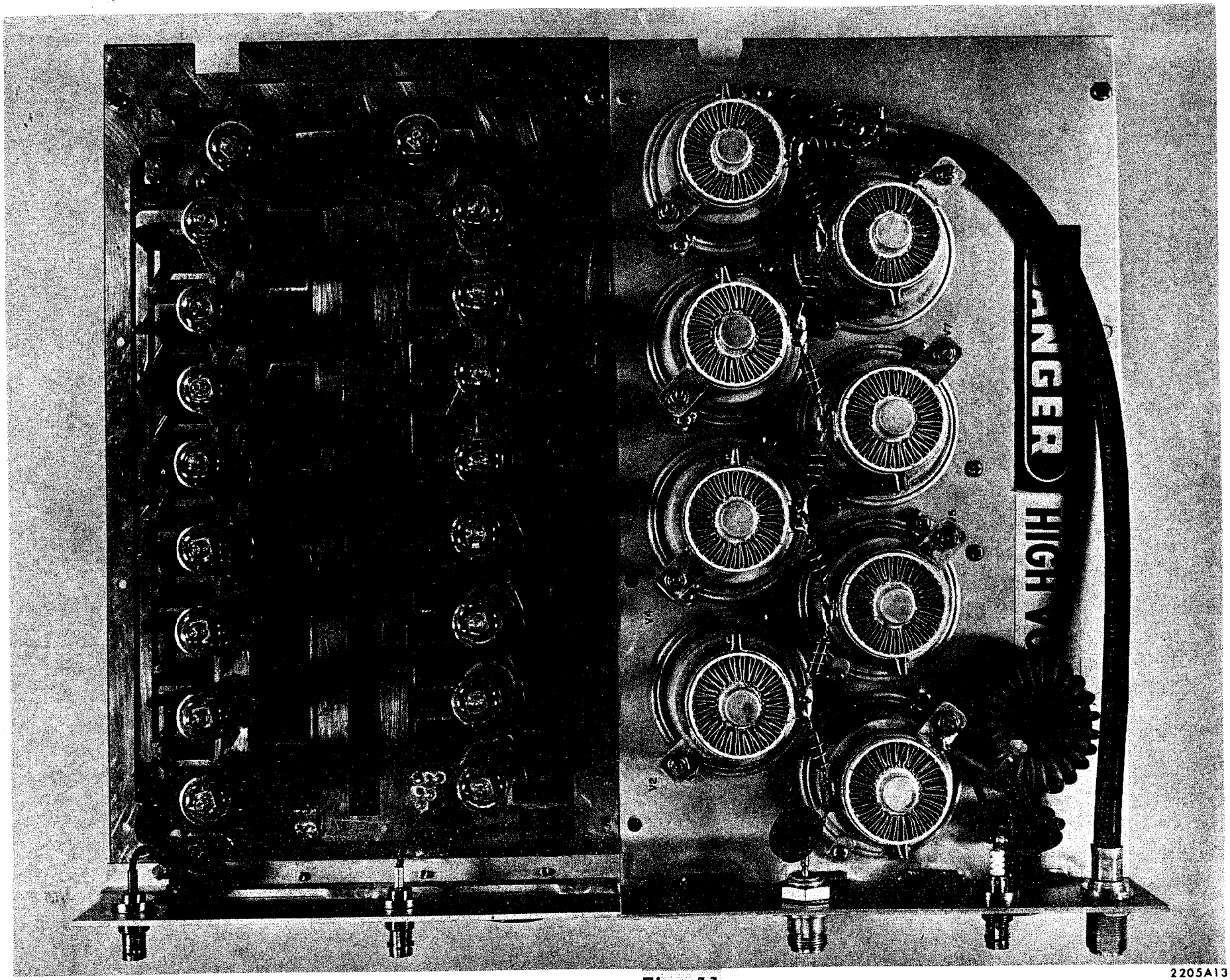

2205A13

Fig. 11

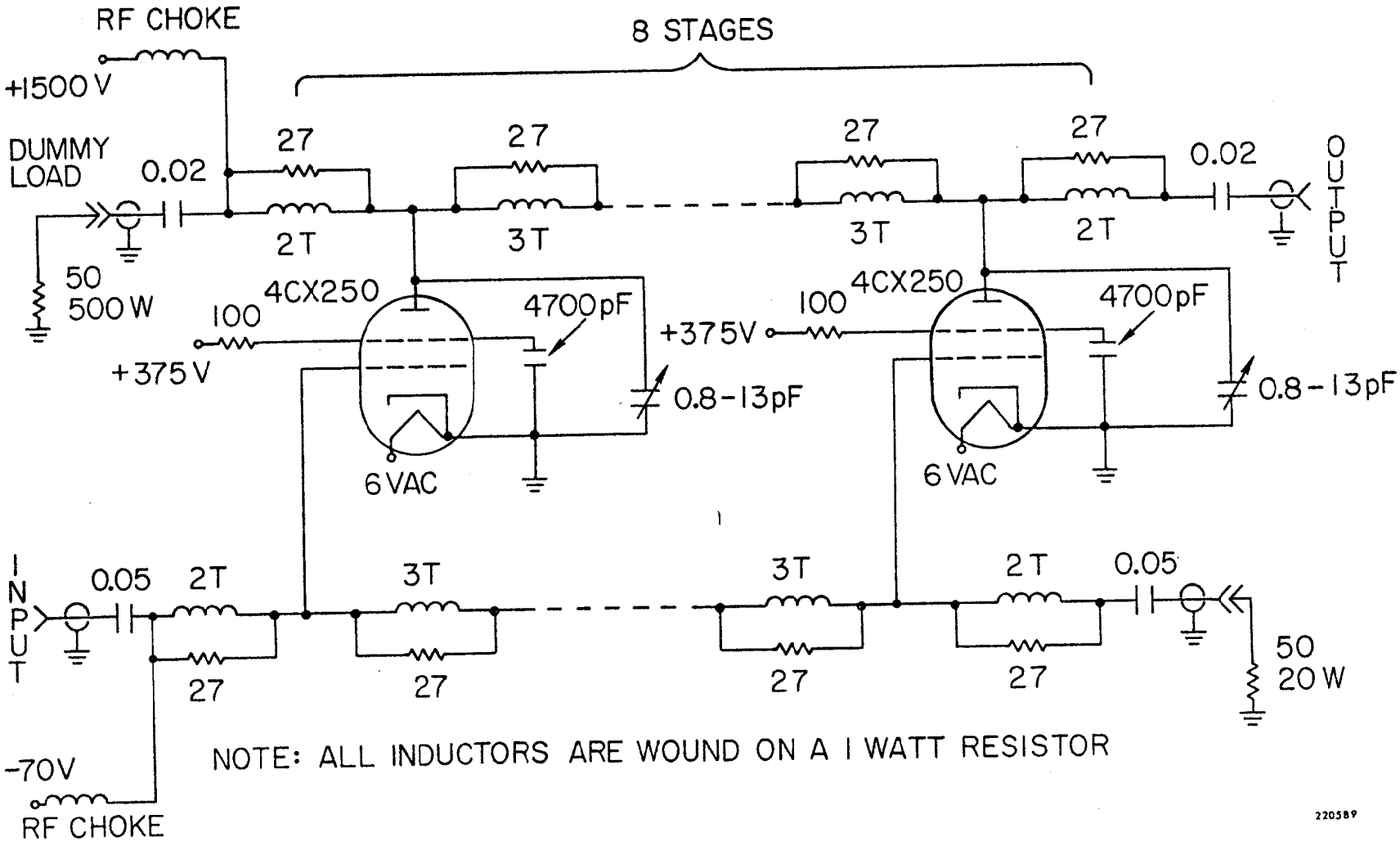
RF CHOKE
+1500 V
8 STAGES
DUMMY LOAD
0.02
27
27
27
27
0.02
OUTPUT
2T
3T
3T
2T
50
500 W
100
4CX250
4700pF
100
4CX250
4700pF
+375 V
+375V
0.8-13pF
0.8-13pF
6 VAC
6 VAC
INPUT
0.05
2T
3T
3T
2T
0.05
27
27
27
27
50
20 W
-70V
RF CHOKE
NOTE: ALL INDUCTORS ARE WOUND ON A 1 WATT RESISTOR
220589

Fig. 12

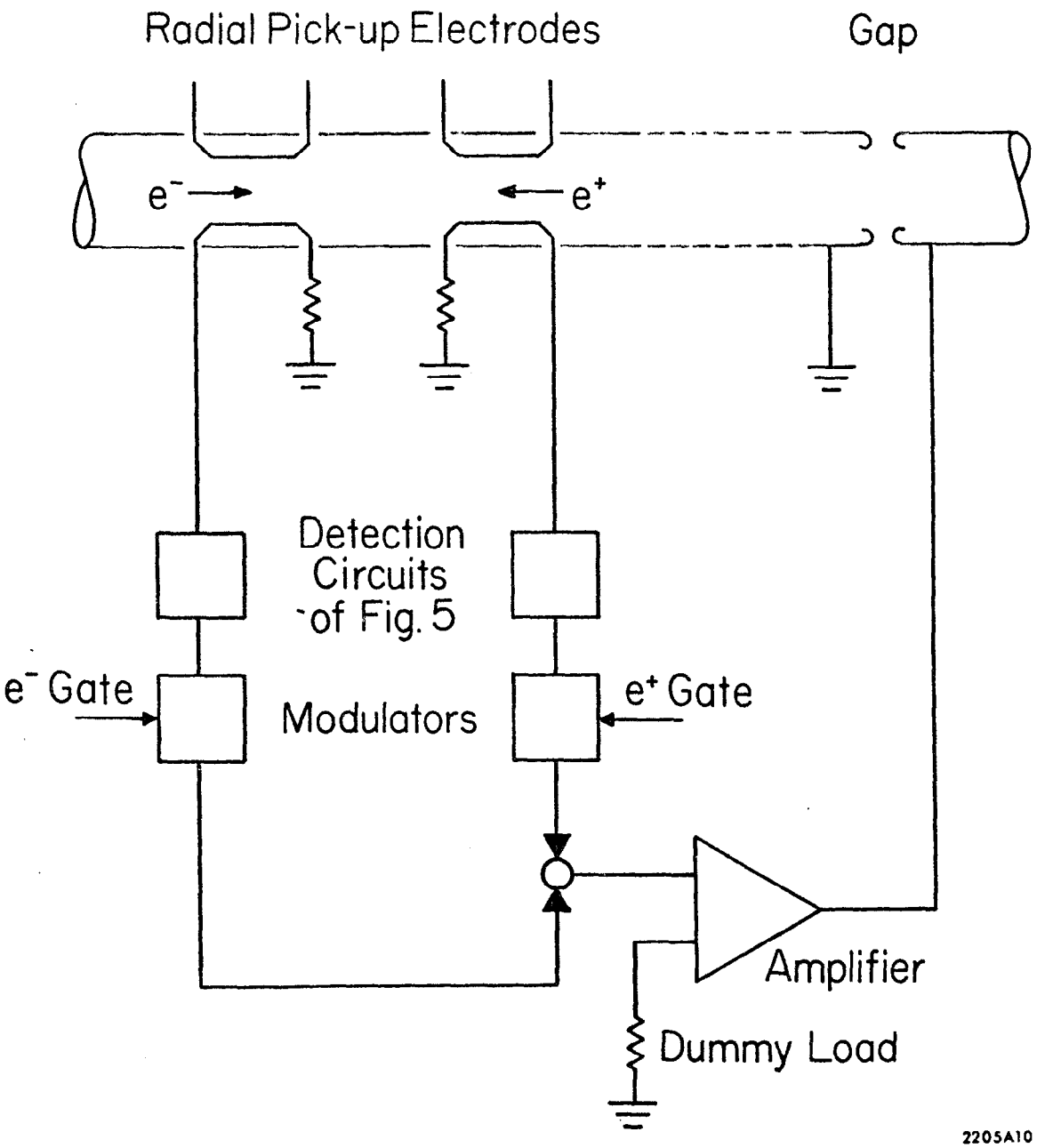
Radial Pick-up Electrodes
Gap
e⁻
e⁺
Detection
Circuits
of Fig. 5
e⁻ Gate
Modulators
e⁺ Gate
Amplifier
Dummy Load
2205A10

Fig. 13

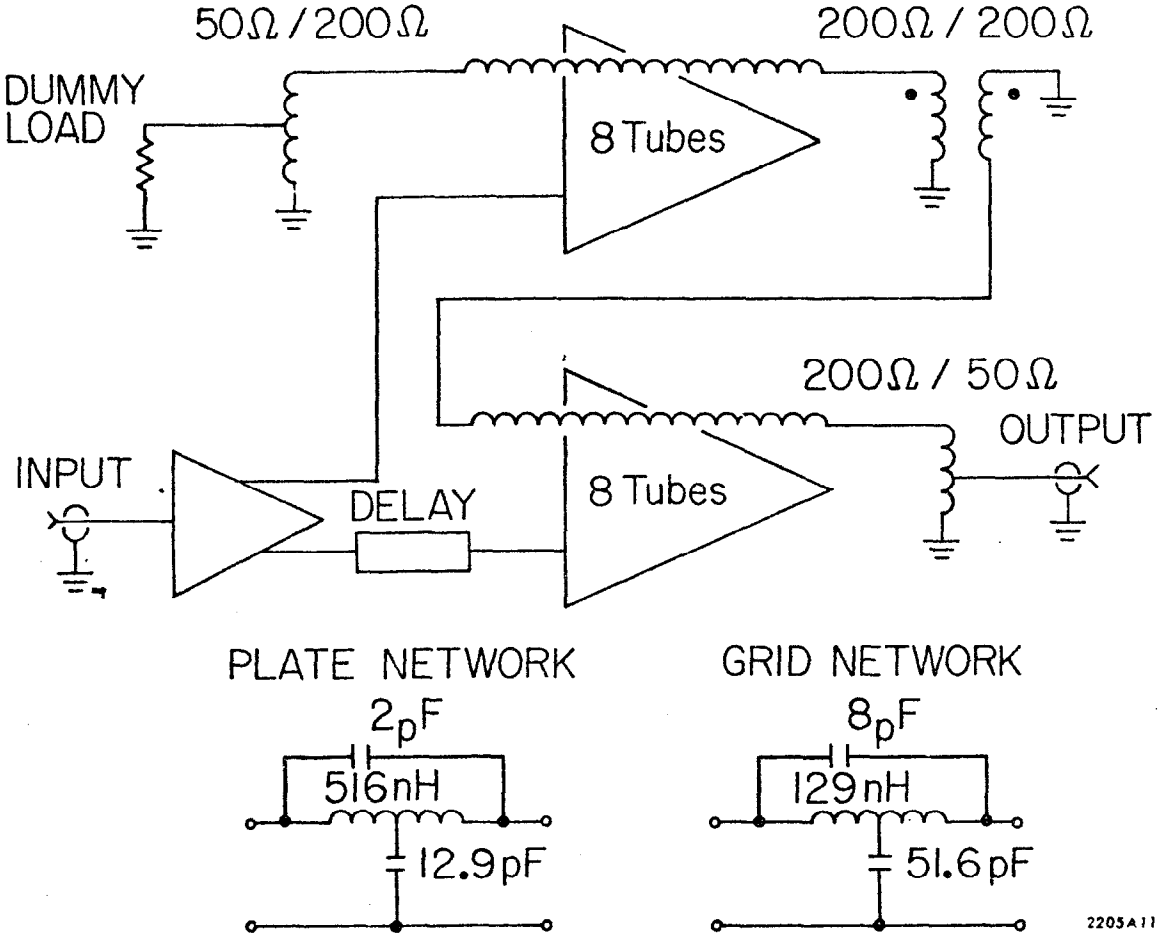
50Ω / 200Ω
200Ω / 200Ω
DUMMY LOAD
8 Tubes
200Ω / 50Ω
OUTPUT
INPUT
DELAY
8 Tubes
PLATE NETWORK
2pF
516nH
12.9pF
GRID NETWORK
8pF
129nH
51.6pF
2205A11

Fig. 14

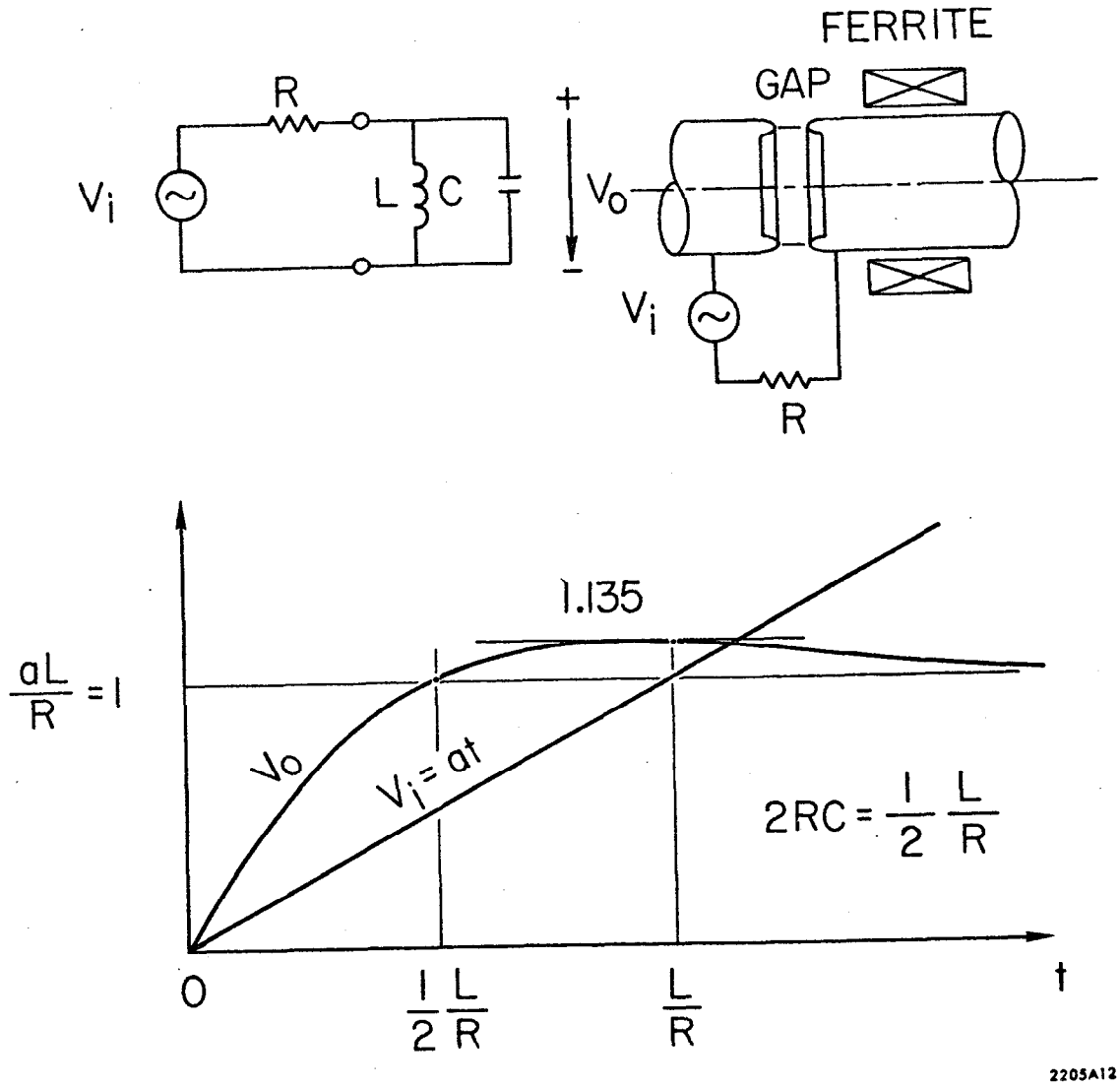
FERRITE
GAP
R
L
C
V_i
+
V_o
V_i
R
1.135
$\frac{aL}{R} = 1$
V_o
$V_i = at$
$2RC = \frac{1}{2}\frac{L}{R}$
0
$\frac{1}{2}\frac{L}{R}$
$\frac{L}{R}$
t
2205A12

Fig. 15